Chemical Science

ROYAL SOCIETY OF CHEMISTRY

EDGE ARTICLE

View Article Online
View Journal | View Issue



Cite this: *Chem. Sci.*, 2024, **15**, 1068

All publication charges for this article have been paid for by the Royal Society of Chemistry

# Photoexcitation of (diarylmethylene)amino benziodoxolones for alkylamination of styrene derivatives with carboxylic acids†

Daichi Okumatsu,[a] Kensuke Kiyokawa, *[a] Linh Tran Bao Nguyen,[b] Manabu Abe *[b] and Satoshi Minakata *[a]

Received 14th November 2023
Accepted 12th December 2023

DOI: 10.1039/d3sc06090j

rsc.li/chemical-science

The alkylamination of alkenes using pristine carboxylic acids was achieved by the photoexcitation of (diarylmethylene)amino benziodoxolones (DABXs), which serve as both an oxidant and an aminating reagent (an iminyl radical precursor). The developed method is a simple photochemical reaction without the need for external photosensitizers and shows a broad substrate scope for aliphatic carboxylic acids leading to the formation of primary, secondary, and tertiary alkyl radicals, thus enabling the facile synthesis of various structurally complex amines. Mechanistic investigations including transient absorption spectroscopy measurements using a laser flash photolysis (LFP) method disclosed the unique photochemical reactivity of DABXs, which undergoes homolysis of their I–N bonds to give an iminyl radical and *ortho*-iodobenzoyloxy radical, the latter of which participates in the single-electron oxidation of carboxylates.

## Introduction

Nitrogen-containing organic molecules are an important class of compounds that have wide applications in organic synthesis, medicinal chemistry, and material science. Therefore, the development of simple and efficient methods for the synthesis of such compounds is an important research topic. The intermolecular carboamination of readily available alkene feedstocks, in which C–C and C–N bonds are formed simultaneously, is an attractive strategy for the rapid synthesis of structurally complex amines.[1] Although the transition-metal-catalyzed non-annulative carboamination of alkenes, mainly aryl- and alkenylamination, has been successfully developed in this area,[2–7] the method of alkylamination has rarely been explored even though it would further expand the utility of carboamination for the synthesis of various nitrogen-containing organic molecules.[5a,b]

A strategy involving alkyl radical species has emerged as a useful approach for the alkylamination of alkenes (Scheme 1a).[8] Early examples of such reactions required the use of structurally specific alkyl radical precursors such as alkyl nitriles,[9] α-halocarbonyl compounds,[10] and perfluoroalkyl halides[11] (Scheme 1b). Although alkylborane derivatives have recently been utilized as alkyl radical precursors,[12,13] they still lack availability and versatility in terms of introducing the desired alkyl group. As a general alkyl radical precursor, aliphatic carboxylic acids are highly attractive because they are stable, non-toxic, and ubiquitous in Nature.[14] Despite these advantages, due to their relatively high redox potential, the difficulty of selectively oxidizing carboxylic acids to generate alkyl radicals in the presence of more readily oxidized amines prevents their direct use in alkylamination reactions. Therefore, existing methods rely on the use of preactivated carboxylic acid derivatives with a higher oxidation state. For example, alkylamination reactions using diacyl peroxides[15] or redox-active esters[16] through a single electron reduction by a transition metal or a photoredox catalyst have been reported. Most recently, an elegant reaction system was reported by Glorius, in which a bifunctional oxime ester serves as both an alkyl radical and a nitrogen-centered radical through a photo-induced triplet energy transfer mechanism.[17,18] However, these methods require additional steps for the preparation of alkyl radical precursors, which reduces the efficiency of the net reaction, and the use of appropriate catalysts. In order to realize a more straightforward alkylamination using pristine carboxylic acids, a new strategy employing a suitable aminating reagent and an oxidant that allows single-electron oxidation of carboxylic acids should be explored (Scheme 1c).

Our group previously developed (diarylmethylene)amino benziodoxolones (DABXs) as a unique oxidative aminating reagent that functions as a single-electron oxidant as well as an

[a]*Department of Applied Chemistry, Graduate School of Engineering, Osaka University, Yamadaoka 2-1, Suita, Osaka 565-0871, Japan. E-mail: kiyokawa@chem.eng.osaka-u.ac.jp; minakata@chem.eng.osaka-u.ac.jp*

[b]*Department of Chemistry, Graduate School of Advanced Science and Engineering, Hiroshima University, Kagamiyama 1-3-1, Higashi-hiroshima, Hiroshima 739-8526, Japan. E-mail: mabe@hiroshima-u.ac.jp*

† Electronic supplementary information (ESI) available. CCDC 2286656–2286658. For ESI and crystallographic data in CIF or other electronic format see DOI: https://doi.org/10.1039/d3sc06090j

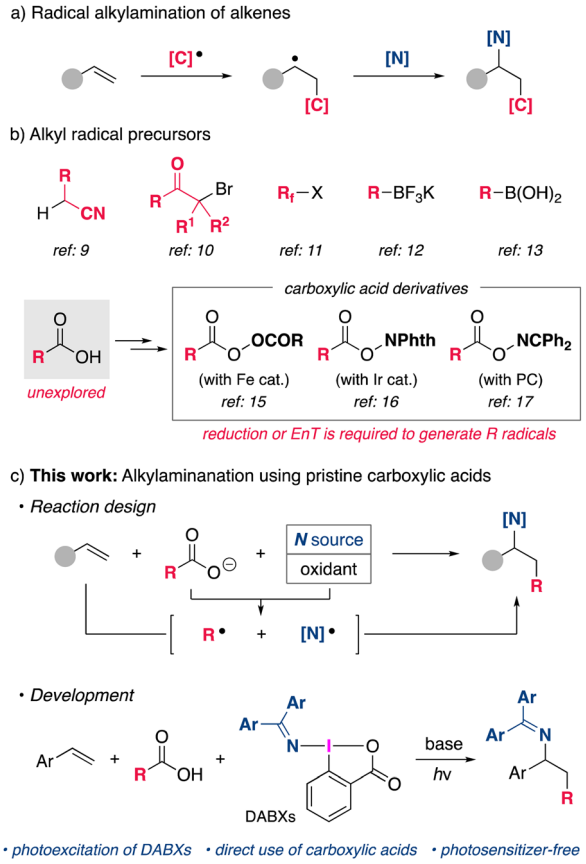


Scheme 1 Radical alkylamination of alkenes initiated by carbon-centered radicals.

iminyl radical source.[19] Accordingly, we envisioned that DABXs would be promising bifunctional reagents that could oxidize a carboxylate and simultaneously generate an alkyl radical and an iminyl radical species, which would then participate in the regioselective alkylamination of alkenes (Scheme 1c). Herein, we report on a new types of reactivity of DABXs that proceeds under conditions of photoirradiation, enabling the intermolecular alkylamination of styrene derivatives with simple carboxylic acids. The developed photochemical reaction proceeds effectively without the need for external photosensitizers.

## Results and discussion

### Reaction development

Our initial efforts focused on the alkylamination of methyl 2-(*p*-tolyl)acrylate (**1a**) with 1-methylcyclohexane-1-carboxylic acid (**2a**) and DABX **3a** in DMSO in the presence of $K_2CO_3$ (Scheme 2). However, the target reaction without irradiation did not proceed well even under the heating conditions (entries 1 and 2). Indeed, a cyclic voltammetry (CV) measurement of **3a** indicated that the reduction potential of **3a** (−1.52 V *vs.* SCE in $CH_2Cl_2$)[19a] is not sufficient to oxidize the carboxylate (*ca.* +1.2 V *vs.* SCE). We then turned our attention to the photoirradiation conditions because photoexcited molecules generally behave as a better oxidant (reductant) than those in the ground state.[20] Waser recently reported that the excitation of ethynylbenziodoxolones (EBXs) with visible light increases their oxidation ability.[21] The UV-vis spectrum of **3a** (0.05 M in DMSO) was then measured, and the results showed a weak absorption in the visible light region. Based on this result, the use of a violet LED (390 nm) was examined, and, under these conditions, the alkylamination proceeded efficiently to give the desired **4** in 82% yield (entry 3). A brief screening of the wavelength of the light source revealed that the yield of **4** increased to 92% when a blue LED (467 nm) was used (entry 4), while the use of a green LED (525 nm) resulted in a very low yield of the product (entry 5). It should be noted that the present alkylamination features a photosensitizer-free reaction.

The reaction conditions including bases, solvents, and aminating reagents were then surveyed (Table 1). The alkylamination reaction also proceeded with almost the same efficiency when $Na_2CO_3$ and $Cs_2CO_3$ were used instead of $K_2CO_3$ (entries 2 and 3). In the absence of $K_2CO_3$, the yield of the product was significantly decreased, indicating that the formation of a carboxylate is necessary to promote the reaction (entry 4). Examining the reaction in other polar solvents showed that DMSO was suitable for this alkylamination (entries 5 and 6). Other oxidative aminating reagents were also investigated. The use of the benziodoxole-based reagent **5** resulted in the low efficiency, suggesting the importance of a benziodoxolone scaffold in **3a** (entry 7). The *O*-aryl oxime **6** was also found to be unsuitable for this reaction (entry 8).[22] The use of the oxime ester **7** and the *O*-sulfonyl oxime **8**, which are used as electrophilic aminating reagents,[23] failed to afford the target product (entries 9 and 10).

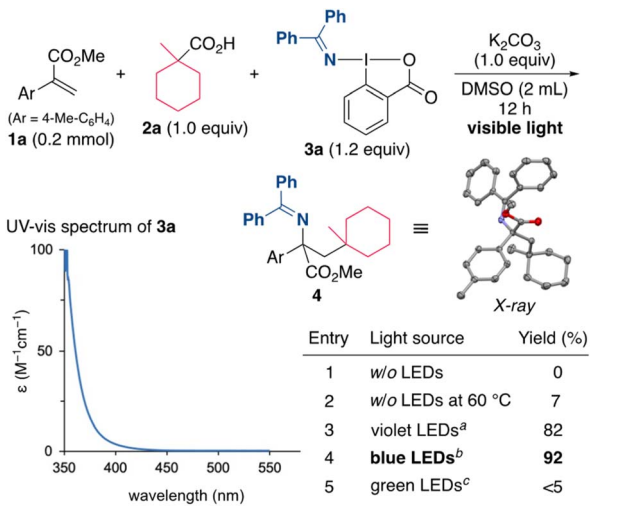


| Entry | Light source | Yield (%) |
|---|---|---|
| 1 | *w/o* LEDs | 0 |
| 2 | *w/o* LEDs at 60 °C | 7 |
| 3 | violet LEDs[a] | 82 |
| 4 | **blue LEDs**[b] | **92** |
| 5 | green LEDs[c] | <5 |

Scheme 2 Initial studies on the alkylamination. Under the light irradiation conditions, the reaction temperature within the reaction vial was maintained around 27 °C. (Left bottom) UV-vis absorption spectrum of **3a** (0.05 M in DMSO). [a] Kessil PR160L 390 nm (max 40 W). [b] Kessil PR160L 467 nm (max 40 W). [c] Kessil PR160L 525 nm (max 40 W).

Table 1 Survey of bases, solvents, and aminating reagents[a]

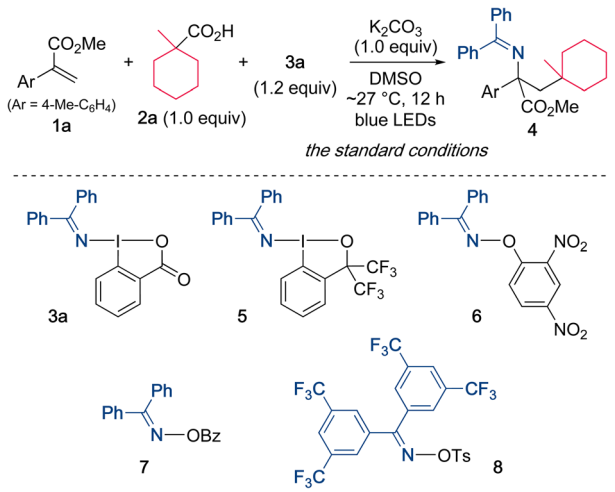


| Entry | Variation from the standard condition | Yield[b] (%) |
|---|---|---|
| 1 | None | 92 (84)[c] |
| 2 | $Na_2CO_3$ instead of $K_2CO_3$ | 92 |
| 3 | $Cs_2CO_3$ instead of $K_2CO_3$ | 87 |
| 4 | Without $K_2CO_3$ | 18 |
| 5 | MeCN instead of DMSO | 32 |
| 6 | DMF instead of DMSO | 78 |
| 7 | **5** (1.0 equiv.) instead of **3a** | 17 |
| 8 | **6** (1.0 equiv.) instead of **3a** | 15 |
| 9 | **7** (1.0 equiv.) instead of **3a** | 0 |
| 10 | **8** (1.0 equiv.) instead of **3a** | 0 |

[a] Reactions were performed on a 0.2 mmol scale (0.1 M) under irradiation using Kessil PR160L 467 nm (max 40 W). The reaction temperature within the reaction vial was maintained around 27 °C. [b] Determined by $^1$H NMR analysis of the crude product using 1,1,1,2-tetrachloroethane as an internal standard. [c] Isolated yield on a 0.4 mmol scale.

## Substrate scope and synthetic utility

With the optimized reaction conditions in hand, the scope of alkylamination was next explored (Scheme 3). In initial experiments, a series of 2-arylacrylates bearing both electron-donating and electron-withdrawing groups on the aryl moiety were subjected to the alkylamination, and all of the reactions proceeded effectively to afford the corresponding products in good to high yields (Scheme 3A, **9–16**). Several functional groups including halogens (**9–12**) and a trifluoromethyl group (**14**) on the aromatic ring were well tolerated. The presence of a substituent at the *ortho* and *meta*-positions had little effect on the reaction efficiency in the formation of **17** and **18**, respectively. Substrates bearing a 3,4-methylenedioxyphenyl group also readily participated in the alkylamination (**19**). These reactions using 2-arylacrylates as substrates provided unnatural α-amino acid derivatives containing α-tertiary carbon centers, which are otherwise difficult to access. In addition, an α,β-unsaturated ketone (**20**), 1,1-di(hetero)arylethenes (**21** and **22**), and styrene derivatives (**23** and **24**) were also applicable for use in this alkylamiantion.

Subsequently, the scope of carboxylic acids for the alkylamination was then investigated (Scheme 3B). A wide range of carboxylic acids bearing an α-quaternary carbon center could be applied to the present alkylamination, thus allowing the introduction of bulky alkyl groups (**25–28**). A carboxyl group on the aromatic ring was found to be inert toward decarboxylation under the oxidative conditions, leading to the chemoselective formation of **28**. Notably, three-dimensional scaffolds with carbon skeletons such as adamantyl (**29**), bicyclo[2.2.2]octyl (**30**), cubyl (**31**), and bicyclo[1.1.1]pentyl (**32**) groups, which are of great interest as bioisosteres of the phenyl ring in medicinal chemistry,[24] could be successfully introduced. Substrates containing oxa and aza-heterocycles were also well tolerated (**33** and **34**). An α-NHBoc (**35**) and an α-hydroxy (**37**) carboxylic acids could also be used as alkylating reagents, and using the latter provided γ-lactone **36** through an intramolecular cyclization of the alkylaminated product **37**. The synthetic utility of this alkylamination was also demonstrated by a gram-scale synthesis of **35** without any loss of yield (1.21 g, 84%). Furthermore, carboxylic acids leading to secondary and primary alkyl radicals were compatible with the alkylamination, allowing the introduction of various alkyl groups including five and six-membered heterocyclic scaffolds (**38–45**). In particular, the product **43** with an unprotected hydroxy group was synthesized by using L-serine. Finally, the scope of DABXs was surveyed (Scheme 3C). Derivatives containing electronically varied imine moieties could be used to deliver the corresponding products **46–51**, indicating that this alkylamination was not significantly influenced by the electronic property of the (diarylmethylene) amino group albeit the yields were somewhat lower for reactions using electron-rich reagents (**48** and **49**). An unsymmetrical (diarylmethylene)amino group could also be introduced (**51**).

To further expand the scope of the alkylamination, the method was applied to electron-deficient alkenes. The reaction using acrylonitrile as a substrate under the standard conditions resulted in the production of only trace amounts of the target product. A brief screening of solvents and bases revealed that the use of acetone and KOAc could promote the alkylamination (Scheme 4). The reaction of acrylonitriles with **2l** and **3a** in the presence of KOAc in acetone under irradiation conditions proceeded effectively, affording **52** and **53**. The use of a violet LED (390 nm) instead of a blue LED (467 nm) was able to significantly shorten the reaction time. In addition, acrylates were also subjected to alkylamination to afford the corresponding amines **54** and **55** in moderate yields. These results further extend the utility of the present alkylamination method for the synthesis of various nitrogen-containing organic molecules. However, simple aliphatic alkenes are unsuccessful substrates,[25] probably due to the slow rate of the addition of alkyl radicals to aliphatic alkenes.[26]

The synthetic utility of the present alkylamination was further highlighted by the derivatization of the products (Scheme 5). The facile transformation of the (diphenylmethylene)amino group of the product was demonstrated by acid hydrolysis and hydride reduction of the crude product of **25**, affording α-amino ester **56** and diphenylmethylamine **57**,

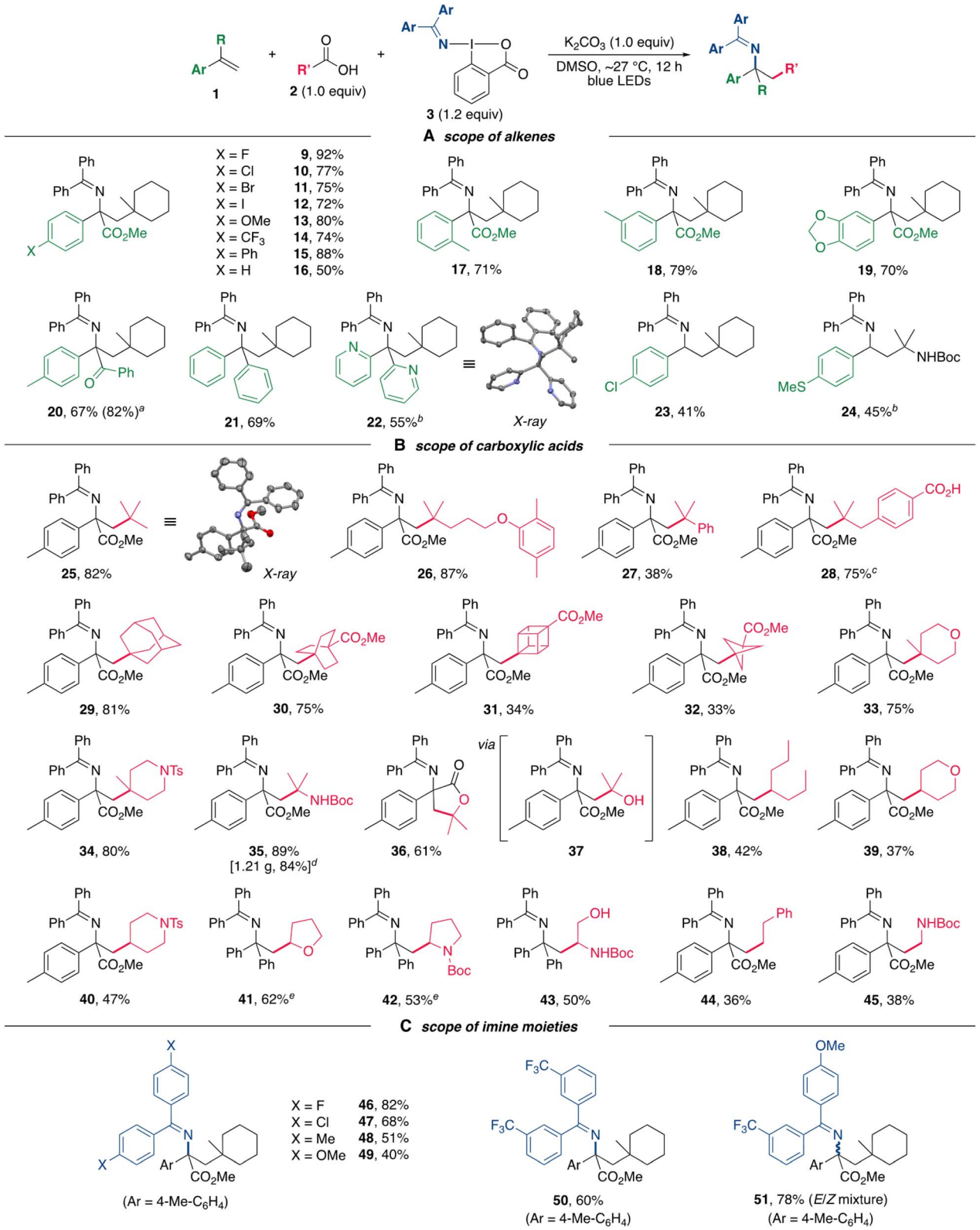


Scheme 3 Scope for alkylamination. Reactions were performed on a 0.2–0.4 mmol scale (0.1 M) under irradiation using Kessil PR160L 467 nm (max 40 W). The reaction temperature within the reaction vial was maintained around 27 °C. Yields are isolated yields. [a] Determined by $^1$H NMR analysis of the crude product. [b] **2** (2.0 equiv.), **3** (2.0 equiv.), and $K_2CO_3$ (2.0 equiv.) were used. [c] The product was isolated as the corresponding methyl ester. [d] Reaction was conducted on a 2.8 mmol scale. [e] **2** (1.2 equiv.), **3** (1.2 equiv.), and $K_2CO_3$ (1.2 equiv.) were used.

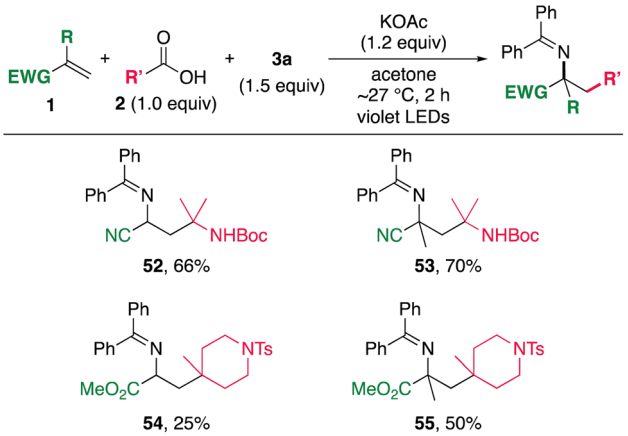


Scheme 4 Alkylamination of electron-deficient alkenes. Reactions were performed on a 0.2 mmol scale (0.07 or 0.03 M). Under irradiation using Kessil PR160L 390 nm (max 40 W). The reaction temperature within the reaction vial was maintained around 27 °C. Yields are isolated yields.

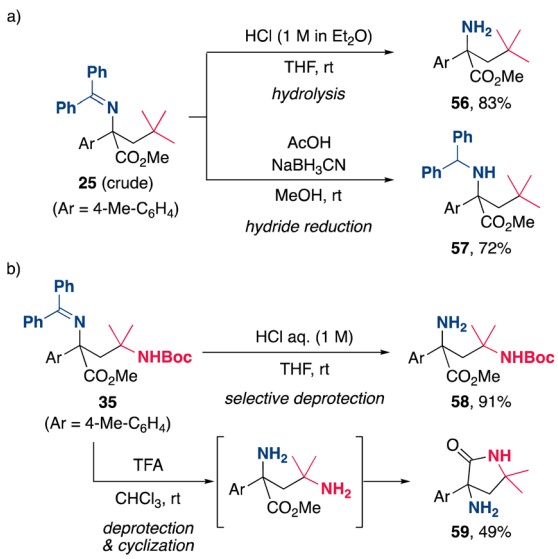


Scheme 5 Transformations of alkylaminated products: hydrolysis and hydride reduction.

respectively, in good yields (Scheme 5a). Furthermore, the chemoselective hydrolysis of the imine moiety of **35** was achieved by the treatment with aqueous HCl to provide **58** in excellent yield (Scheme 5b). Hydrolysis of both amino functionalities of **35** using trifluoroacetic acid (TFA) provided a diamine, which subsequently underwent cyclization to yield the γ-lactam **59**, a key structural motif in pharmaceuticals and natural products. These quite simple methods provide efficient and practical processes for the synthesis of a variety of useful nitrogen-containing organic molecules.

## Mechanistic investigations

Mechanistic aspects of the alkylamination were investigated. The possibility of the ligand exchange reaction between **3a** and

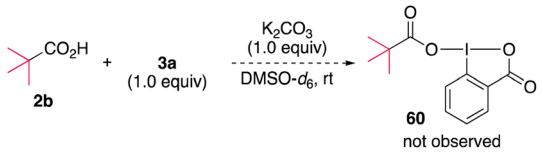


Scheme 6 NMR monitoring of a mixture of **2b** and **3a**.

carboxylate to form the carboxylate-substituted hypervalent iodine compound was initially examined. When a mixture of pivalic acid (**2b**) and **3a** in the presence of $K_2CO_3$ in DMSO-$d_6$ was monitored by $^1$H NMR (Scheme 6), no new signals were observed, and the starting materials remained, ruling out the possibility of ligand exchange (see ESI, Fig. S3†). In addition, density functional theory (DFT) calculations of the ligand exchange process at the M06-2X/6-311++G(d,g)-SDD(I) level of theory indicated that the formation of **60** is thermodynamically unfavorable ($\Delta G$ = +2.1 kcal mol$^{-1}$), consistent with the experimental results. We next examined the possibility that an electron donor–acceptor (EDA) complex was formed between a carboxylate and DABXs. The UV-vis spectrum of the reaction mixture was nearly superimposable over that of **3a** (see ESI, Fig. S4†), ruling out the participation of a photoactive EDA complex in the reaction. Based on these results, we conclude that DABXs would be directly excited and initiate the reaction.

To investigate the photochemical reactivity of DABX **3a**, a series of experiments and quantum chemical calculations were performed. A fluorescence emission analysis of **3a** was first conducted in DMSO at room temperature. No significant emission signal was observed under these conditions (see ESI, Fig. S5†), suggesting that the singlet electronically excited state is chemically reactive, and/or that the intersystem crossing process is fast to produce the triplet state.[27] We then conducted sub-microsecond transient absorption (TA) spectroscopy measurements of **3a** in DMSO using a laser flash photolysis (LFP) method (266 nm or 355 nm Nd/YAG-laser, 12 ns pulse-width, 10 Hz, 6 mJ per pulse) to gain insights into the transient species generated during the photolysis of **3a** (Scheme 7a). After the LFP, a transient species absorbing at 350–600 nm with $\lambda_{max}$ ~ 410 nm was observed under air in DMSO at 298 K. The decay time-profile monitored at 420 nm could not be reproduced by a single exponential decay-equation. The half-life ($\tau_{1/2}$) was ~6.8 μs at 298 K under an atmosphere of air. Under an argon atmosphere, the similar $\tau_{1/2}$ was found to be ~6.6 μs at 298 K, indicating that the transient species with $\lambda_{max}$ ~ 410 nm is not quenched by molecular oxygen ($O_2$). These experimental results clearly suggest that the triplet excited state of **3a** is not the transient species with $\lambda_{max}$ ~ 410 nm. Interestingly, the structural optimization of triplet state of **3a** at the UB3LYP/6-31G(d)-LanL2DZ(I) level of theory produced a pair of radicals, a diphenyl iminyl radical **61a** and *ortho*-iodobenzoyloxy radical (**62**), suggesting that the triplet **3a** spontaneously generates the radical pair after the I–N bond homolysis. In addition to the generation of the transient with $\lambda_{max}$ ~ 410 nm, the bleaching signal at ~300 nm and its recovering process with $k_{rec}$ = 2.13 × 10$^{10}$ M$^{-1}$ s$^{-1}$ were observed in the LFP experiments (see ESI,

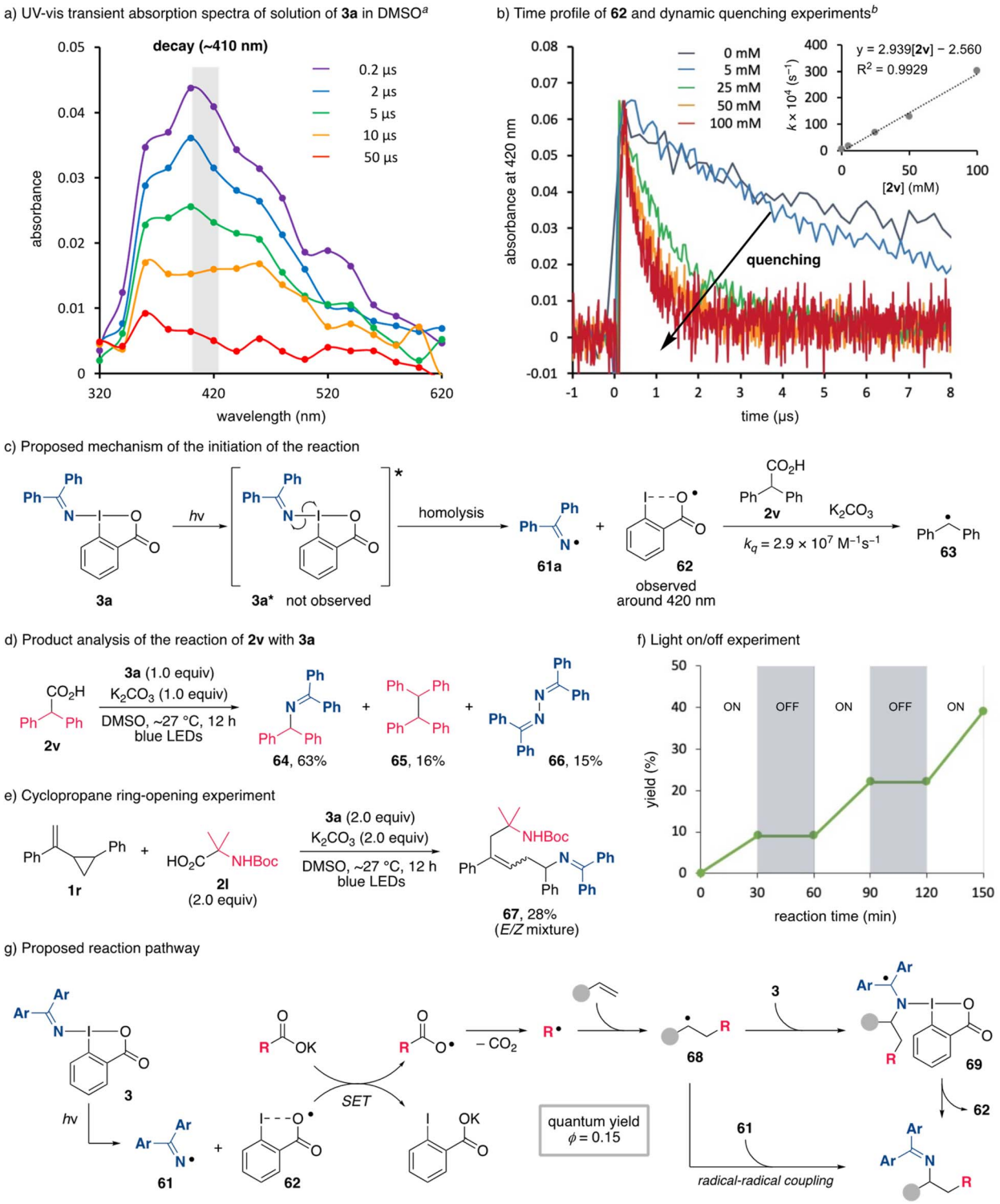


Scheme 7 Mechanistic investigations and proposed reaction mechanism. (a) Sub-microsecond transient absorption spectra of $1.7 \times 10^{-4}$ M solution of **3a** in DMSO under air. (b) The time profile is obtained from transient ultraviolet-visible spectra of $2.6 \times 10^{-2}$ M solution of **3a** in DMSO under air. Stern–Volmer plot is obtained from rate constants observed at different concentration of **2v** at 420 nm.

Fig. S7†). The rise in the signal is attributed to the recovering process of **3a** from the pair of radicals.

The absorption spectra of **61a** and **62** were computed using time-dependent density functional theory (TD-DFT) calculations at the UB3LYP/6-31G(d)-LanL2DZ(I) level of theory. The computational method well reproduced the absorption spectrum of compound **3a** (see ESI, Fig. S9†). Thus, we applied the method to simulate the absorption spectra of **61a** and **62**.

Weak electronic transitions at 491 nm ($f = 0.0025$, $\varepsilon = \sim 100$), 353 nm ($f = 0.015$, $\varepsilon = \sim 1300$), and 337 nm ($f = 0.018$, $\varepsilon = \sim 1300$) were computed for iminyl radical **61a**, where $f$ is the oscillator strength; $\varepsilon$ is molar extinction coefficient in $M^{-1}\ cm^{-1}$ (see ESI, Fig. S10†). For radical **62**, a weak transition at 758 nm ($f = 0.027$, $\varepsilon = \sim 1100$) and a relatively strong one at 463 nm ($f = 0.125$, $\varepsilon = \sim 5000$) were found over 300 nm at the same level of theory (see ESI, Fig. S11†). The computed results clearly suggest that the observed transient absorption at $\lambda_{max} \sim 410$ nm in the LFP experiments of **3a** is derived from radical **62**. In addition, the peroxyl radical **62**_$O_2$ was not optimized as an equilibrated structure to give a weakly bounded complex of radical **62** and $O_2$ during the structural optimization in the doublet state, suggesting that the reaction of **62** with $O_2$ is endothermic and slow. Indeed, the Gibbs energy of the complex was computed to be higher in energy by 5.8 kcal $mol^{-1}$ than the total energy of **62** and $O_2$ (see ESI, Fig. S13†). This computational result also supports the conclusion that the transient absorption with $\lambda_{max} \sim 410$ nm comes from radical **62**, since the transient species with $\lambda_{max} \sim 410$ nm was not quenched by $O_2$. Unfortunately, the signal of **61a** could not be clearly obtained due to the low $\varepsilon$ and the overlap with the absorption spectra of **3a** and **62**.

As mentioned above, the decay process of **62** was not reproduced by the first-order decay equation. However, the experimentally observed decay-signal at 420 nm was perfectly reproduced with the second-order rate equation (**61a** + **62** → **3a**, $[\mathbf{62}] = 1/(kt + 1/[\mathbf{62}]_0)$, where $[\mathbf{62}]_0 = [\mathbf{61a}]_0 = 3.88 \times 10^{-6}$ M), to give the second-order rate constant ($k$) of $1.7 \times 10^{10}\ M^{-1}\ s^{-1}$ (see ESI, Fig. S8†), supporting the conclusion that assignment of **62** is correct. The initial concentration of **62** was determined by the bleaching signal of **3a** at 300 nm after the LFP, $Abs_{300} = -0.0231$, $\varepsilon_{300}$ of **3a** = 5946.7. The quantitative formation of **62** from **3a** was assumed to determine the concentration.

To understand the thermal reactivity of **62**, we then investigated the dynamic quenching of **62** with the carboxylate prepared from **2v** with $K_2CO_3$ to determine whether it could function as an oxidant (Scheme 7b and c). Indeed, the lifetime ($\tau = 1/k_q$) of **62** was shortened by increasing the concentration of **2v**. From the slope of the Stern–Volmer plot, $k_q$ *versus* [**2v**], the quenching rate constant $k_q$ was found to be $2.9 \times 10^7\ M^{-1}\ s^{-1}$. Unfortunately, the resulting diphenylmethyl radical **63** ($\lambda_{max}$ = 335 nm, $\varepsilon$ 29 900)[28] formed through the fast decarboxylation was not clearly detected, although the lifetime at 370 nm was different from that at 420 nm. The optical window was more than 370 nm for the LFP experiments. To further confirm the single-electron transfer process, the reduction potentials of **61a**, **62**, and a carboxylate of **2v** were then computed using DFT calculations at the M062X/6-31G+(d,g)-LanL2DZ(I) level of theory. Since structural optimization of the carboxyl radical species derived from **2v** resulted in the formation of the diphenylmethyl radical **63** due to the barrierless decarboxylation, the calculations were carried out using a pivalate instead (see ESI†). The resulting reduction potentials for **61a**, **62**, and oxidation potential for a pivalate were −1.12, +1.20, and +1.37 V *vs.* SCE, respectively, indicating that the single-electron oxidation of pivalate by **62** is possible although the electron transfer oxidation is slightly endothermic ($\Delta G_{et}$ = +0.17 eV). Indeed, the estimated quenching rate constant obtained by the Rehm–Weller equation, $\sim 1.8 \times 10^7\ M^{-1}\ s^{-1}$, is fairly consistent with the experimentally obtained value $k_q = 2.9 \times 10^7\ M^{-1}\ s^{-1}$ (*vide supra*).[29]

To confirm the generation of an iminyl radical **61a** as well as the alkyl radical **63**, the product analysis of photochemical reaction of **2v** (0.1 M) with **3a** (0.1 M) was carried out in the presence of $K_2CO_3$ (Scheme 7d). As a result, the decarboxylative amination product **64** was obtained, accompanied by the formation of byproducts including **65** and benzophenone azine (**66**), which are apparently formed through the homocoupling of **63** and **61a**, respectively.[30] These results clearly demonstrate that the generation of **61a** and **63** under the reaction conditions, which would couple to provide **64**. Overall, the excitation of **3a** led to the formation of the iminyl radical **61a** and radical **62** that can oxidize a carboxylate to give an alkyl radical. Although there are several reports on the reactivity of radical **62** as a single-electron oxidant,[31,32] the present study is a rare example of an experimental demonstration of its reactivity.[33] A radical mechanism was further confirmed by the use of vinylcyclopropane **1r** as an alkene substrate (Scheme 7e). When **1r** was subjected to the standard alkylamination reaction conditions, no cyclopropane-containing product was observed, and several cyclopropane ring-opened products were obtained, one of which was determined to be **67**. This result clearly indicates that the reaction proceeds through radical addition of an alkyl radical to an alkene.

Based on the experimental results reported herein, a proposed reaction pathway for the alkylamination is depicted in Scheme 7g. As an initial step, the visible-light excitation of DABXs **3** leads to the homolysis of its I–N bond to give an iminyl radical **61** and radical **62**. A single-electron oxidation of a carboxylate by **62** then occurs. The resulting alkyl radical through a subsequent decarboxylation reacts with alkenes to form radical **68**. Given that the relative concentration of **3** is much higher than that of **61**, the radical **68** would undergo the radical addition onto **3**. The Gibbs energy barrier was then computed to be 32.0 kcal $mol^{-1}$ at the M06-2X/6-31G+(d,g)-LanL2DZ(I) level of theory (see ESI, Fig. S15†). The product and the radical **62** were found to be produced through the formation of the weakly bounded intermediate **69**. The regeneration of radical **62** realizes the radical-chain process. However, the result of the light ON/OFF experiments (Scheme 7f) and the quantum yield $\Phi = 0.15$ of the alkylamination do not support an efficient radical chain process, and continuous photoirradiation is therefore required for the reaction. Therefore, an alternative pathway involving a radical–radical coupling between **68** and iminyl radical **61** cannot be excluded.

## Conclusions

In conclusion, the alkylamination of alkenes using pristine carboxylic acids as an alkylating reagent was enabled by photoexcitation of DABXs which function as both an oxidant and an aminating reagent. The present method has a broad substrate scope for alkenes and aliphatic carboxylic acids with good functional group tolerance. The developed alkylamination

would provide a simple, scalable, and straightforward approach to accessing readily modifiable amines. The synthetic utility of the products was clearly demonstrated by the facile transformation of some of the products into valuable nitrogen-containing molecules. Experimental and computational mechanistic studies revealed the unprecedented photochemical reactivity of DABXs. Upon visible light irradiation, *ortho*-iodobenzoyloxy radical, *in situ*-generated from DABXs, oxidizes carboxylates to provide alkyl radicals. We anticipate that the present method will find wide applications in the synthesis of amines that are otherwise difficult to access.

## Data availability

Experimental procedures, compound characterization data, crystal data, computational details, and NMR spectra can be found in ESI.†

## Author contributions

D. O. performed the main part of the experiments. L. T. B. N. performed the quantum yield experiments. D. O. and K. K. wrote the draft of the manuscript, participated in compound characterization, and ESI† preparation. M. A. and S. M. supervised the research. All authors discussed the results and prepared the manuscript.

## Conflicts of interest

There are no conflicts to declare.

## Acknowledgements

This work was supported by JSPS KAKENHI Grant numbers JP21J20313, JP22H02078, JP22H05362, JP22K19033, JP21H01921, and JST CREST Grant number JPMJCR18R4. K. K. also thanks the research fund of the Asahi Glass Foundation.

## Notes and references

1 X. Chen, F. Xiao and W.-M. He, *Org. Chem. Front.*, 2021, **8**, 5206–5228.
2 T. Piou and T. Rovis, *Nature*, 2015, **527**, 86–90.
3 Z. Hu, X. Tong and G. Liu, *Org. Lett.*, 2016, **18**, 1702–1705.
4 A. Lerchen, T. Knecht, C. G. Daniliuc and F. Glorius, *Angew. Chem., Int. Ed.*, 2016, **55**, 15166–15170.
5 (*a*) Z. Liu, Y. Wang, Z. Wang, T. Zeng, P. Liu and K. M. Engle, *J. Am. Chem. Soc.*, 2017, **139**, 11261–11270; (*b*) V. A. van der Puyl, J. Derosa and K. M. Engle, *ACS Catal.*, 2019, **9**, 224–229; (*c*) T. Kang, N. Kim, P. T. Cheng, H. Zhang, K. Foo and K. M. Engle, *J. Am. Chem. Soc.*, 2021, **143**, 13962–13970; (*d*) T. Kang, J. M. González, Z.-Q. Li, K. Foo, P. T. W. Cheng and K. M. Engle, *ACS Catal.*, 2022, **12**, 3890–3896.
6 (*a*) D. Wang, L. Wu, F. Wang, X. Wan, P. Chen, Z. Lin and G. Liu, *J. Am. Chem. Soc.*, 2017, **139**, 6811–6814; (*b*) D. Wang, F. Wang, P. Chen, Z. Lin and G. Liu, *Angew. Chem., Int. Ed.*, 2017, **56**, 2054–2058.
7 S. Lee and T. Rovis, *ACS Catal.*, 2021, **11**, 8585–8590.
8 H. Jiang and A. Studer, *Chem. Soc. Rev.*, 2020, **49**, 1790–1811.
9 (*a*) Y.-Y. Liu, X.-H. Yang, R.-J. Song, S. Luo and J.-H. Li, *Nat. Commun.*, 2017, **8**, 14720–14725; (*b*) N. Zhu, T. Wang, L. Ge, Y. Li, X. Zhang and H. Bao, *Org. Lett.*, 2017, **19**, 4718–4721.
10 S. N. Gockel, T. L. Buchanan and K. L. Hull, *J. Am. Chem. Soc.*, 2018, **140**, 58–61.
11 Y. Xiong, X. Ma and G. Zhang, *Org. Lett.*, 2019, **21**, 1699–1703.
12 J. J. Kennedy-Ellis, E. D. Boldt and S. R. Chemler, *Org. Lett.*, 2020, **22**, 8365–8369.
13 S. N. Gockel, S. Lee, B. L. Gay and K. L. Hull, *ACS Catal.*, 2021, **11**, 5166–5171.
14 (*a*) J. Xuan, Z.-G. Zhang and W.-J. Xiao, *Angew. Chem., Int. Ed.*, 2015, **54**, 15632–15641; (*b*) J. Schwarz and B. König, *Green Chem.*, 2018, **20**, 323–361.
15 B. Qian, S. Chen, T. Wang, X. Zhang and H. Bao, *J. Am. Chem. Soc.*, 2017, **139**, 13076–13082.
16 X.-H. Ouyang, Y. Li, R.-J. Song and J.-H. Li, *Org. Lett.*, 2018, **20**, 6659–6662.
17 (*a*) T. Patra, P. Bellotti, F. Strieth-Kalthoff and F. Glorius, *Angew. Chem., Int. Ed.*, 2020, **59**, 3172–3177; (*b*) H.-M. Huang, P. Bellotti, J. Ma, T. Dalton and F. Glorius, *Nat. Rev. Chem.*, 2021, **5**, 301–321; (*c*) G. Tan, M. Das, H. Keum, P. Bellotti, C. Daniliuc and F. Glorius, *Nat. Chem.*, 2022, **14**, 1174–1184.
18 For exmples of other carboamination reactions, see:(*a*) Y. Zhang, H. Liu, L. Tang, H. J. Tang, L. Wang, C. Zhu and C. Feng, *J. Am. Chem. Soc.*, 2018, **140**, 10695–10699; (*b*) J. Majhi, R. K. Dhungana, Á. Rentería-Gómez, M. Sharique, L. Li, W. Dong, O. Gutierrez and G. A. Molander, *J. Am. Chem. Soc.*, 2022, **144**, 15871–15878.
19 (*a*) K. Kiyokawa, D. Okumatsu and S. Minakata, *Angew. Chem., Int. Ed.*, 2019, **58**, 8907–8911; (*b*) D. Okumatsu, K. Kawanaka, S. Kainuma, K. Kiyokawa and S. Minakata, *Chem.–Eur. J.*, 2023, **29**, e202203722; (*c*) A. Yoshimura, A. Saito and V. V. Zhdankin, *Adv. Synth. Catal.*, 2023, **365**, 2653–2675.
20 For recent examples, see:(*a*) M. Silvi, E. Arceo, I. D. Jurberg, C. Cassani and P. Melchiorre, *J. Am. Chem. Soc.*, 2015, **137**, 6120–6123; (*b*) Y. Sato, K. Nakamura, Y. Sumida, D. Hashizume, T. Hosoya and H. Ohmiya, *J. Am. Chem. Soc.*, 2020, **142**, 9938–9943.
21 S. G. E. Amos, D. Cavalli, F. Le Vaillant and J. Waser, *Angew. Chem., Int. Ed.*, 2021, **60**, 23827–23834.
22 J. Davies, S. G. Booth, S. Essafi, R. A. W. Dryfe and D. Leonori, *Angew. Chem., Int. Ed.*, 2015, **54**, 14017–14021.
23 H. Tsutsui, T. Ichikawa and K. Narasaka, *Bull. Chem. Soc. Jpn.*, 1999, **72**, 1869–1878.
24 M. A. M. Subbaiah and N. A. Meanwell, *J. Med. Chem.*, 2021, **64**, 14046–14128.
25 For a list of unsuccessful substrates, see ESI†
26 H. Fischer and L. Radom, *Angew. Chem., Int. Ed.*, 2001, **40**, 1340–1371.
27 For a example of a direct $S_0 \rightarrow T_n$ transition in the photoreaction of hypervalent iodine compounds,

see:M. Nakajima, S. Nakagawa, K. Matsumoto, T. Kuribara, A. Muranaka, M. Uchiyama and T. Nemoto, *Angew. Chem., Int. Ed.*, 2020, **59**, 6847–6852.

28 (*a*) G. Porter and M. W. Windsor, *Nature*, 1957, **180**, 187–188; (*b*) L. M. Hades, M. S. Platz and J. C. Scarano, *J. Am. Chem. Soc.*, 1984, **106**, 283–287.

29 S. Farid, J. P. Dinnocenzo, P. B. Merkel, R. H. Young, D. Shukla and G. Guirado, *J. Am. Chem. Soc.*, 2011, **133**, 11580–11587.

30 (*a*) T. Okada, M. Kawanishi and H. Nozaki, *Bull. Chem. Soc. Jpn.*, 1969, **32**, 2981–2983; (*b*) A. R. Forrester, M. Gill and J. S. Sadd, *J. Chem. Soc., Chem. Commun.*, 1975, 291–292.

31 (*a*) G.-X. Li, C. A. Morales-Rivera, Y. Wang, F. Gao, G. He, P. Liu and G. Chen, *Chem. Sci.*, 2016, **7**, 6407–6412; (*b*) G.-X. Li, C. A. Morales-Rivera, F. Gao, Y. Wang, G. He, P. Liu and G. Chen, *Chem. Sci.*, 2017, **8**, 7180–7185; (*c*) F. Le Vaillant, M. D. Wordrich and J. Waser, *Chem. Sci.*, 2017, **8**, 1790–1800.

32 For examples of the use of an iodanyl radical as a H-atom transfer reagent, see:(*a*) M. Ochiai, T. Ito, H. Takahashi, A. Nakanishi, M. Toyonari, T. Sueda, S. Goto and M. Shiro, *J. Am. Chem. Soc.*, 1996, **118**, 7716–7730; (*b*) S. A. Moteki, A. Usui, T. Zhang, C. R. S. Alvarado and K. Maruoka, *Angew. Chem., Int. Ed.*, 2013, **52**, 8657–8660; (*c*) J. Jiang, R. Ramozzi, S. Moteki, A. Usui, K. Maruoka and K. Morokuma, *J. Org. Chem.*, 2015, **80**, 9264–9271.

33 (*a*) B. L. Frey, M. T. Figgins, G. P. Van Trieste, R. Carmieli and D. C. Powers, *J. Am. Chem. Soc.*, 2022, **144**, 13913–13919; (*b*) A. Maity, B. L. Frey and D. C. Powers, Iodanyl Radical Catalysis, *Acc. Chem. Res.*, 2023, **56**, 2026–2036.